Thermodynamic Evaluation of Low-GWP and Environmentally Friendly Alternative Refrigerants

Mahmood H. Khaleel[1], Mohammad S. Hassan[1], Otabeh Al-Oran[2], Salwa O. Mohammed[1] & Sherwan Mohammed Najm[1]

[1] Kirkuk Technical Institute, Northern Technical University, Kirkuk, 36001, Iraq

[2] Renewable Energy Technology Department, Applied Science Private University, Amman, 11937, Jordan

Correspondence: Sherwan Mohammed Najm, Kirkuk Technical Institute, Northern Technical University, Kirkuk, 36001, Iraq. E-mail: sherwan@ntu.edu.iq

Abstract

Refrigerant systems, crucial for modern life, are increasingly important due to their environmental impact and rising energy costs, with their advancement influenced by social life evolution and widespread use in homes and buildings. A systematic search using thermodynamic models identified 48 possible ternary mixtures and 5 pure refrigerants. These combinations, based on thermodynamics, could provide energy savings, paving the way for real-world testing and definitive conclusions, not yet studied in literature. REFPROP refers to the reference fluid properties program, developed by NIST version 9.0 for 2010, is a program for calculating the thermodynamic and transport properties of industrially important fluids and their mixtures. This program was used to evaluate the refrigerant properties in different mixing ratios. Then, using the MATLAB version of 2020 apparatus to arrange and solve all the variables to generate the results under set boundary conditions, all the characteristics were incorporated into thermodynamic equations. when compared to R134a, the results demonstrated that mixtures of natural refrigerants usually have acceptable thermal performance; these mixtures may be recommended as suitable replacements for refrigeration and air conditioning systems because they are environmentally harmless and have a low GWP.

Keywords: refrigerant mixture, alternative refrigerant, GWP and ODP

1. Introduction

In recent years, due to their environmental impact and increasing energy costs, energy conservation and the environmental safety of refrigeration systems have become worldwide concerns (Al-Oran et al.,2024). The advancement of refrigeration systems specifically depends on the evolution of social life, which has made these systems an integral part of modern life. Because of their use in a variety of everyday situations, these systems can be found in nearly every building and house. It's important to note that global energy demand is expected to be around 30 and 46 Terawatt (TW) by 2050 and 2100, respectively (Sahaym & Norton, 2008). Renewable energy has huge interest and is expected to provide 50% of the world's energy by 2040, and it can play a crucial role in reducing gas emissions to the environment by about 70% during 2050. Convenient energy sources supply more than 90% of our energy requirements but at a greater environmental cost. For example, in the last 150 years, the concentration of carbon dioxide in the environment has risen from 280 to 370 ppm. Even by the end of the century, it is predicted to reach 550 ppm (Lund, 2007). It was criticized for the size of the banks as well as their contribution to total European emissions up to 2030, and it will project a rapid decrease. In the last five years of the analysis period, emissions were close to zero (Karlsson et al., 2020; Graziosi et al., 2015) As well as studying the addition of nano-sized materials for the purpose of improving the thermal performance of fluids and the possibility of improving their thermal properties for the purpose of reducing the energy spent for industrial, domestic, and other purposes (Hamadalla et al., 2023; Kamel & Najm, 2020). In recent years, the primary motivations for research have been ozone depletion, global warming, and efficient energy usage. Because of the need for alternatives to traditional CFC and HCFC refrigerants, refrigerant mixtures have been considered as alternatives. In addition to replacing environmentally damaging pure fluid refrigerants, potential thermodynamic cycle benefits also exist (Nawaz et al., 2017; Khaleel et al., 2018; McLinden et al., 2020; Gebbie et al., 2004; Khalifaa et al., 2017). The use of natural refrigerants, such as hydrocarbons, is one of the best strategies for

resolving energy and environmental problems in the refrigeration industry. Hydrocarbons have no ODP and an extremely low GWP. In general, hydrocarbons increase energy efficiency by 10-15% in various refrigeration and air-conditioning applications. Despite these benefits, hydrocarbon refrigerants have been banned in standard refrigeration and air-conditioning applications for several decades because of safety concerns. However, due to an environmental mandate, this trend has decelerated somewhat in recent years. As a result, some flammable refrigerants have been used in specific applications (Yang et al., 2021; Park & Jung, 2009). Theoretical investigation into the performance of a vapor compression refrigeration system using HFC and HC blends as replacements for the refrigerant R22. All of the investigated refrigerant mixtures are ozone-friendly in nature, with GWPs ranging from 0.0244 to 1.685 times that of R22 in window air conditioners with R431A, R410A, R419A, R134a, R1270, and R290, and fifteen refrigerant mixtures consisting of R134a, R1270, and R290. The results show that the COP for the refrigerant mixture R134a/R1270/R290 (50/5/45 by mass percentage) is 2.10% higher than that of R22, R431A, R410A, R419A, R134a, R1270, and R290, with compressor discharge temperatures 4.8oC to 22.2oC lower than that of R22 and power consumption per ton of refrigeration (Shaik & Babu, 2017). New low-GWP refrigerants are being developed to replace conventional, higher-GWP refrigerants. HFO-1123/HFC-32 and HFO-1123/HFC-32/HFO-1234yf showed azeotropic-like behavior and the potential to be an alternative to R-410A when used in domestic and commercial air conditioners. According to the analysis, these new refrigerants perform similarly to conventional refrigerants (Hashimoto et al., 2019). The search for alternative refrigerants to hydrocarbons has not been considered, but the experimental investigations found in the literature indicate that there is room for improvement. Accordingly, the objective of this work is to present the results of a thermodynamic screening of refrigerant mixtures that could be 'better' refrigerants or at least reduce the energy consumption of stand-alone systems based on R-600a or R-290 and to analyze if thermodynamically the hypothesis is possible due to their low global warming potential (GWP) and zero ozone depletion potential (ODP) (Reddy et al., 2016; Calleja-Anta et al., 2020). Thus, a systematic search based on thermodynamic models was carried out, with many mixing ratios considered for possible ternary mixtures under different performance conditions, yielding a total of 48 combinations as well as 5 pure refrigerants. This evaluation yielded a small number of combinations that, thermodynamically, could provide energy savings. As a result, based on the authors' knowledge, this new line of research will allow the scientific community to test the proposed mixtures in real-world systems and draw definitive conclusions that have not been studied in the literature.

2. Refrigeration Categorizations and Thermodynamic Frameworks

The vapor compression refrigeration cycle is made up of four component parts: the compressor, the condenser, the expansion valve, and the evaporator (Rostamzadeh et al., 2018). It is a compression technique intended to increase the pressure of the refrigerant as it flows from an evaporator. The high-pressure refrigerant flows through a condenser before going back to the evaporator at the initial low pressure. A more thorough outline of the steps is offered below:

Heat is transferred from the refrigerant to the surrounding environment. As the refrigerant flows through the condenser at constant pressure, it expands and releases pressure as it enters the expansion tool. As a consequence, the temperature drops at this stage. As a result of these transformations, the refrigerant exits the expansion tool as a liquid-vapor mixture. Expansion tools satisfy two significant roles in the vapor compression cycle. First, they keep a pressure differential between the low- and high-pressure sides. Second, they regulate how much liquid refrigerant enters the evaporator. The refrigerant, in this case, is at a lower temperature than its surroundings. As a result, it evaporates and absorbs vaporization's latent heat. At low pressure and temperatures, heat is extracted from the refrigerant. The suction effect of the compressor aids in maintaining the low pressure (Wang, 1994). A schematic diagram of a vapor compression refrigeration system with a sub-cooling heat exchanger is shown in **Figure1** (Bolaji, 2014).

Geometrically designed properties were tested on a single evaporator domestic refrigerator of 10-ft^3 (0.283 m^3) using capillary tube lengths of 4m for household refrigerators based on the best result obtained from experimental data by M. Fatouh (2018) (Fatouh, 2018).
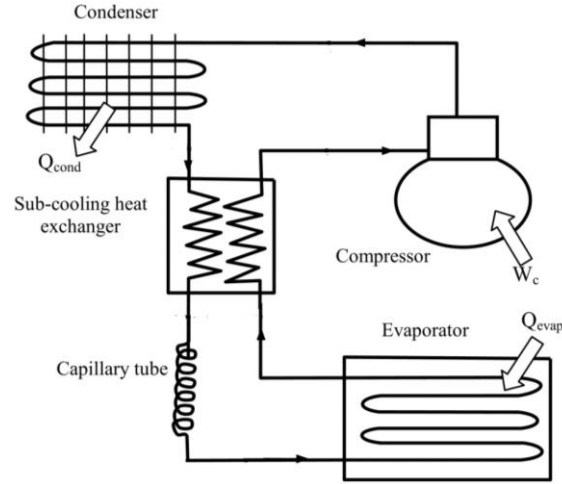
Figure 1. Refrigeration system with a sub-cooling heat exchanger (Bolaji, 2014).

3. Evaluation of refrigerant mixtures

The abbreviation REFPROP refers to the reference fluid properties program. The National Institute of Standards and Technology (NIST version 9.0 for 2010) created this program for calculating the thermodynamic and transport properties of industrially important fluids and their mixtures. REFPROP was developed on the most accurate pure fluid and mixture models currently available. It incorporates three models for the thermodynamic properties of pure fluids: equations of state explicit in Helmholtz energy, the modified Benedict-Webb-Rubin equation of state, and an extended corresponding states (ECS) model (Ewl et al., 2018).

The process of adiabatic mixing will be analyzed. As shown in **Figures 2-a** and **b**, two binary mixture streams, m_A of mixture A and m_B of mixture B, are adiabatically mixed to make a new mixture stream.

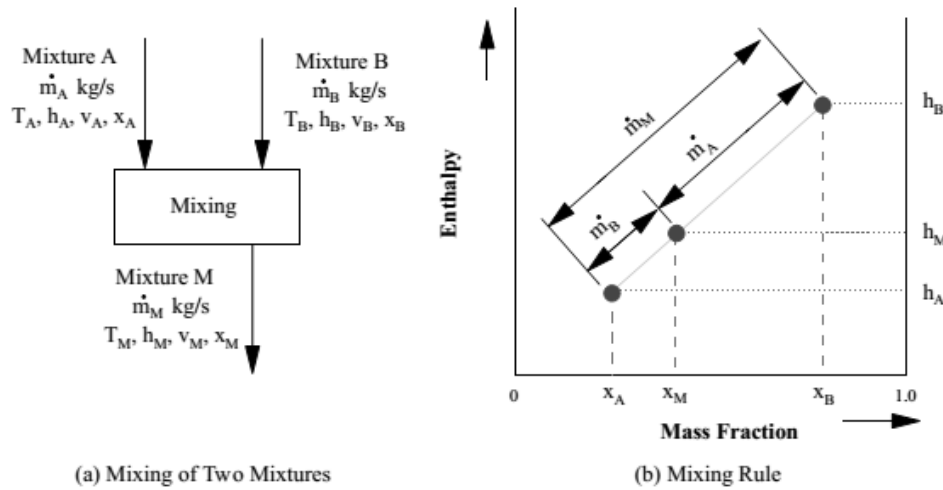(a) Mixing of Two Mixtures   (b) Mixing Rule

Figure 2: Analyzing of adiabatic mixing process

Three conservation equations result from the mass and energy balances:

$$\dot{m}_M = \dot{m}_A + \dot{m}_B \tag{1}$$

$$\dot{m}_M X_M = \dot{m}_A X_A + \dot{m}_B X_B = \dot{m}_M X_A + \dot{m}_B (X_B - X_A) \tag{2}$$

$$\dot{m}_M h_M = \dot{m}_A h_A + \dot{m}_B h_B = \dot{m}_M h_A + \dot{m}_B (h_B - h_A) \tag{3}$$

The mass fraction (x_M) and enthalpy (h_M) of the mixture after mixing can be written as **Equations (4)** and **(5)**. **Equations (1), (2)**, and **(3)** represent the conservation of total mass, species, and energy, respectively.

$$h_M = h_A + \frac{\dot{m}_B}{\dot{m}_M}(h_B - h_A) \tag{4}$$

$$X_M = X_A + \frac{m_B}{m_M}(X_B - X_A) \tag{5}$$

The mean enthalpy is used to calculate the evaporation and condensation pressures (Pe and Pv), which correspond to the evaporating and condensation temperature levels.

$$h_{e \; or \; c \,,m} = \frac{h_{e,in} - h_{e,out}}{2} \tag{6}$$

$$P_{e \; or \; c} = \mathfrak{f}(T_{e \; or \; c}, h_m) \tag{7}$$

The evaporator and condenser outlet temperatures were calculated using **Eqs. (8)** and **(9)**, considering saturation temperatures at the corresponding pressure, the degree of superheat in the evaporator, and the degree of sub-cooling in the condenser.

$$T_{e \,,out} = \mathfrak{f}(T_{e \,,Pe}, +\text{SH}) \tag{8}$$

$$T_{c \,,out} = \mathfrak{f}(T_{c \,,Pc}, -\text{SUB}) \tag{9}$$

3.1 Performance -Analyzing Parameters

The following parameters were investigated to analyze the performance of the tested refrigerant mixtures based on the thermodynamic states of the refrigerants throughout the cycles:

$$COP = \frac{h_{e,out} - h_{e,in}}{h_{c,in} - h_{suc}} \tag{10}$$

3.2 Global Warming Potential (GWP)

Mixture GWP, which is evaluated using **Eq. (11)** as the sum of the partial masses of each refrigerant multiplied by their GWP, is extracted from the 4th Assessment Report of the IPCC (Corr, 1995).

$$GWP = \sum_i^n (m_i \cdot GWP_i) \tag{11}$$

4. Properties of Refrigerants and Boundary Conditions

Table 1 shows the thermodynamic properties of R134a, R513A, R600a, R290, R436A, and R1234yf refrigerants. To obtain comparisons between refrigerants, a theoretical analysis was initially performed.

There is no limit to the relationships that can be used in the mixture based on the GWP values. According to ASHRAE categorization, most of them are flammable, and depending on the composition, mixtures may represent lower flammability than R600a and R290 as pure refrigerants. A single-stage ideal vapor compression refrigeration cycle was implemented in this research. The following assumptions motivate the analyses summarized in **Table 2**.

Table 1. Pure natural refrigerant consideration

Properties / refrigerants	R1234yf	R134a	R600a	R290	R513A	R436A
GWP	4	1260	1	0.02	554	3
ODP	0	0	0	0	0	0
Critical pressure(MPa)	3.38	4.06	3.63	4.25	3.767	4.27
Critical temperature(C)	94.8	101.21	134.81	96.89	96.5	116.04

The refrigerants were examined and compared at set evaporating and condensing temperatures for the cycles under consideration (conditions are shown in **Tables 2** and **3**).

Table 2. Working conditions for the household refrigerator cycle

Working conditions				
Boundary conditions	Te	Tc	SUB	SH
Boundary condition -1-	-15°C	40°C	3°C	5°C
Boundary condition -2-	-25°C	45°C	1°C	4°C

Table 3. Refrigerants properties extraction

Extraction of the property values.				
Thermodynamic proses	Compression proses procedure			
Adiabatic proses	$h_{2s}=f(P_{cv}, S_2=S_1)$	$S_1=f(P_{ev}, T_1)$	$T_1=f(T_{ev}+\text{SUB})$	SUB=f (boundary conditions Table1
Non-adiabatic proses	$h_2=f(\varepsilon ,h_{2s})$	$\varepsilon=80\%$	-	

5. Steps of Working Fluid Evaluation and Study Assumptions

The thermodynamic characteristics of the vapor compression refrigeration cycle in domestic refrigerators have been investigated. Comparing cycle performance with various base (pure) refrigerants (R134a, R600a, R290, and R1234yf and their blends), the purpose of the optimization process is to identify refrigerant mixtures with the best energy performance and compare them to commonly used and must-be-replaced refrigerants (R134a) in the four working conditions considered and shown in **Table 1**, so R134 will be the performance baseline in **Table2**. This study's significant approach was based on the refrigerant working fluid, which consisted of four cases of pure refrigerants. The weight ratio mixtures of these fluids were subsequently identified in order to generate 8 cases, for a total of 12 cases investigated. The research cases were reduced to 24 by employing two types of operating conditions (for the instances of freezing and deep freezing, the evaporation temperatures in the evaporators were -15 and -25 C, and the condensing temperatures in the condenser were 40 and 45 C). To obtain more objective details, two types of compression processes, adiabatic and non-adiabatic (Ɛ=80 %) compression performance, were employed in the compressor, leading to a total of 48 research cases (see Table A1)

6. Energy Performance Analysis

The compressor, condenser, capillary tube, and evaporator are the four basic components of the vapor-compression refrigeration system analysis. These four components are assumed to operate continuously in steady-state behavior. For a simple thermodynamic analysis of the refrigeration system, changes in the kinetic and potential energy of the refrigerant are not considered because they are so small compared to the interactions between work and heat transfer. With this streamlined approach, the steady flow energy equation may be used to evaluate the refrigerant-side refrigeration capacity of the evaporator.

$$Q_e = m(h_1 - h_4) \tag{12}$$

Eq. (12) evaluates the refrigeration capacity for the refrigerant side and the refrigerant enthalpies at the evaporator's output (h_1) and inlet (h_4).

Both adiabatic and non-adiabatic compression processes allow for the evaluation of the refrigerant's compressor power:

$$W_c = m(h_2 - h_1) \tag{13}$$

$$W_{c,s} = m(h_{2s} - h_1) \tag{14}$$

Where h_{2s} denotes the enthalpy at the compressor's exit point in the constant entropy process see **Table 3**. The specific power consumption of refrigeration systems is an invaluable indicator of their energy performance. This is reported by Dalkilic and Wongwises (2010) (Dalkilic & Wongwises, 2010):

Power per ton of refrigeration (PPTR):

$$PPTR = \frac{3.5 \, w_c}{Q_e} \tag{15}$$

The VCRS's coefficient of performance (COP) is given by:

$$COP = \frac{Q_e}{W_c} = \frac{h_1 - h_4}{h_2 - h_1} \, or \, \frac{h_1 - h_4}{h_{2s} - h_1} \tag{16}$$

Using the MATLAB version for 2020 program, calculations are made for all equations, thermal properties are taken into account, and variables are eliminated in accordance with the study plan to obtain the results that are required based on the operational and boundary conditions. This is done after using the REFPRO program to obtain the properties of pure and mixed refrigerants. See **Appendix A**'s **Tables A1, A2, A3, A4**, and **A5**.

7. Mass Flow Rate Calculation

Capillary tube-suction line heat exchangers are commonly used in small refrigeration systems to enhance energy efficiency and ensure that the compressor receives vapor-phase refrigerant. Researchers have looked into the mass flow rate of a refrigerant that flows through a lateral capillary tube suction line heat exchanger and found different empirical correlations (Rasti et al., 2017).

Many geometrical and operational variables affect the mass flow of refrigerant through a capillary tube. First, geometrical conditions include the total length of the capillary tube, the length of the heat exchanger, the adiabatic entrance length, the inner diameter of the capillary tube, and the inner diameter of the suction line (see **Table 6**) (Fatouh, 2018). Secondly, the capillary tube inlet pressure, suction line inlet pressure, capillary tube inlet sub-cooling or refrigerant quality, and suction line inlet superheat temperature were the most important

operating parameters (as well as refrigerant properties). Furthermore, the latent heat of vaporization, specific volume, viscosity, specific heat, and capillary tube inlet enthalpy were all significant parameters of the refrigerant moving through the capillary tube and suction line; all these can be expressed by equation **(18)** (Ewl et al., 2018):

$$\dot{m} = f(L_c, L_i, L_{hx}, D_c, D_s, P_s, x, \mu, \vartheta, c_p, h_{fg}, h_c, \Delta T_{sh}) \tag{17}$$

The dimensionless parameters in π-terms were developed by performing the dimensional analysis and using the Buckingham Pi (π) theorem; these π-terms are listed in **Table 4**. The dimensionless mass flow rate may alternatively be stated as: (Fatouh, 2018)

$$\pi_m = 7.6793 \pi_a^{-0.5741} \pi_b^{0.0186} \pi_c^{0.8174} \pi_d^{-0.1733} \pi_e^{-0.9577} \pi_f^{-0.0383} \pi_g^{-0.0913} \tag{18}$$

Table 4. π-term formulations and descriptions

π-term	Parameters	Description	π-term	Parameters	Description
$\boldsymbol{\pi_a}$	$\dfrac{L_c}{D_c}$	Capillary tube length and inside diameter effect	π_e	$1 + \dfrac{h_{c,in} - h_f}{h_{fg}}$	Enthalpy effect of capillary tube inlet
$\boldsymbol{\pi_b}$	$\dfrac{D_s}{D_c}$	Suction-pipe inside diameter effect	π_f	$\dfrac{\Delta T_{sh} C_{pfc} D_c^2}{\mu_{fc}^2 \vartheta_{fc}^2}$	Superheated temperature effect of suction line inlet
$\boldsymbol{\pi_c}$	$\dfrac{P_{c,in} D_c^2}{\mu_{fc}^2 \vartheta_{fc}}$	Pressure effect of capillary tube inlet	π_m	$\dfrac{\dot{m}}{D_c \mu_{fc}}$	Refrigerant mass flow rate
$\boldsymbol{\pi_d}$	$\dfrac{P_{s,in} D_c^2}{\mu_{fc}^2 \vartheta_{fc}}$	Pressure effect of suction line inlet	π_g	$\dfrac{h_{fgc} D_c^2}{\mu_{fc}^2 \vartheta_{fc}^2}$	Enthalpy of vaporization effect of the capillary tube

Table 5. Operational refrigerant properties

Parameters	Units	Description	Parameters	Units	Description
μ_{fc}^2	Pa.s	Saturated liquid viscosity at Tc,in	$h_{c,in}$	Jkg^{-1}	Inlet enthalpy at Pc,in&Tc,in
ϑ_{fc}	M^{3}kg^{-1}	Saturated vapor specific volume at Tc,in	h_f	Jkg^{-1}	Saturated liquid enthalpy at Pc,in
C_{pfc}	Jkg^{-1}k^{-1}	Saturated liquid specific heat at Tc,in	h_{fg}	Jkg^{-1}	Enthalpy of vaporization at Pc,in

Table 6. Geometric refrigerator parameters

Parameters	Values (m)	Description	Parameters	Values	Description
$\mathbf{D_c}$	0.78 ×10^{-3}	Capillary tube inside diameter	P$_{c,in}$(Pa)	P∫(i, Tc) :i=case(1to48)	Capillary tube inlet pressure
$\mathbf{L_c}$	4	Capillary tube total length	P$_{s,in}$(Pa)	∫(i, Ts) :i=case(1to48)	Suction line inlet pressure
$\mathbf{D_s}$	6.5×$^{-3}$	Suction tube inside diameter	ΔT_{sh}(k)	4 or 5	Superheated temperature
$\mathbf{L_i}$	0.5	Capillary tube inlet adiabatic length	T$_{ci}$(k)	310 or 317	Capillary tube inlet temperature
$\mathbf{L_{sh}}$	1.9	Capillary tube suction line heat exchanger length	T$_{si}$(k)	252 or 263	Suction line inlet temperature

Review **Appendix B** tables **B1, B2, B3**, and **B4** to see the results of the mass flow rate and the main effects on the equation used to calculate the mass flow rate.

8. Results Discussion

The added benefit of the suggested refrigerant combinations is that they have a lower global warming potential (GWP) than the basic refrigerant (R134a). A specific GWP number for refrigerant fluids that is acceptable cannot be determined, but in general, the lower the value, the better. The GWP values of the main mixes utilized in the tests are shown in Figure 3. Though their values varied, they were always less than the basic refrigerant. At (70/30) wt% (R290R600a), (50/50) wt% (R290R600a), and (30/70) wt% (R290R600a) and R1234yf, this impact is almost nonexistent. Given the growing concern about global warming, it is possible that a certain balance of features, such as low GWP and moderate decreases in heating and cooling capacity, could lead to these

alternative combinations being considered in different heating and air conditioning applications. Even if it comes at the expense of the energy used or the thermal performance factor, thermal and ozone layer depletion.
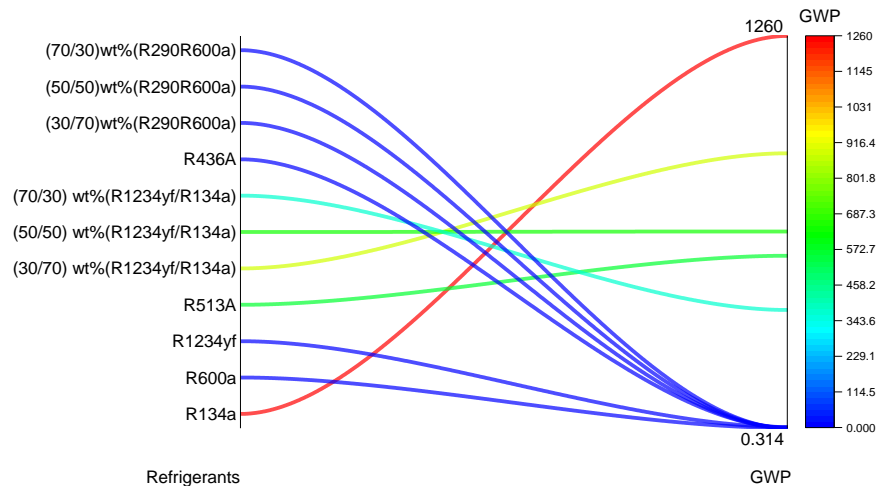

Figure 3. GWP values of the main mixtures utilized in the tests

Figure 4 compares the studied mixtures' cooling capacities to the cooling capacity of the base refrigerant, R134a. The mixtures had a slightly higher cooling capacity than R134a. The mixtures' comparatively high latent heat is the cause, and as a result, a lower flow rate is required for R134a, which implies that less energy is required to provide the same cooling capacity. This results in a reduced rate of energy consumption in the case of R134a for the same cooling capacity. Because they are below deep freezing, the values for boundary condition 2 in **Figure 4b** and boundary condition 1 in **Figure 4a** fluctuate only slightly. This mixing makes the mixtures more efficient at low temperatures. Except for refrigerant 3 (R290), whose results are considered unrealistic because of its very high pressures when charged alone, unless it is mixed with other refrigerants, (8, 10, and 12) record excellent values compared to the basic fluid 1.
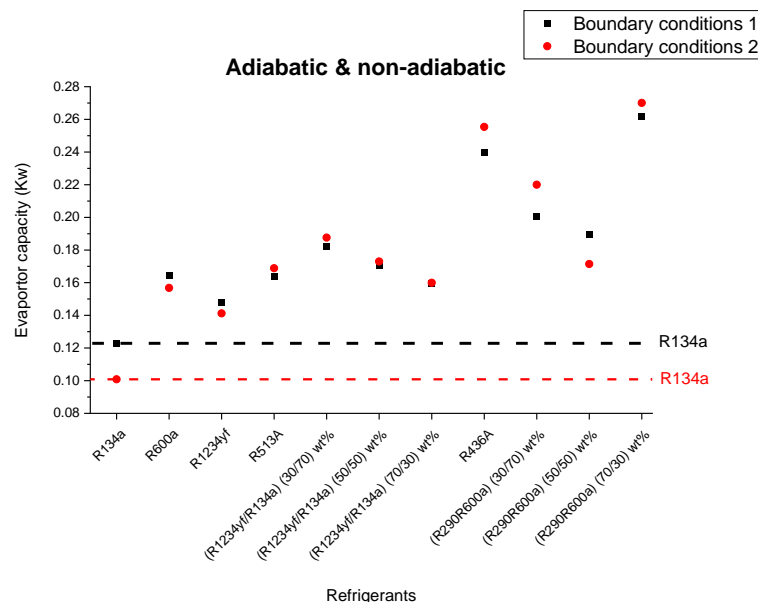

Figure 4. Evaporator capacity - Adiabatic & non-adiabatic - Boundary conditions 1 and 2 for the refrigerant mixture

A variety of mixtures and individual mixtures whose performance was evaluated in a vapor compression refrigeration system are shown in **Figure 5** as having different condensation capacities. The

condensation capacity for boundary condition 1 is shown in **Figure 5a** when the compression process is assumed to be adiabatic, and the condensation capacity for non-adiabatic compression is shown in **Figure 5b**. Because we stated in the **Table 2** that the assumption was constant superheated degrees, it is easy to see how the results would differ if the method were thought of as non-adiabatic. As an example, the mixes (9, 10, 11, and 12) increase at a rate of around 0.2 kW; however, when compared to the base refrigerant, the rate of improvement in the values of Condensing capacity varies between 0.08 and 0.186 kW. The improvement in condensation capacity compared to the base refrigerant 1 ranges between 0.11 and 50.2 kW, and noticeably, the mixtures of natural refrigerants gave good performance in comparison with the base refrigerant 1 in Figures 2c and 2d, which show the condensation capacity of the mixtures under boundary conditions 2 and whether the compression process is adiabatic or not.
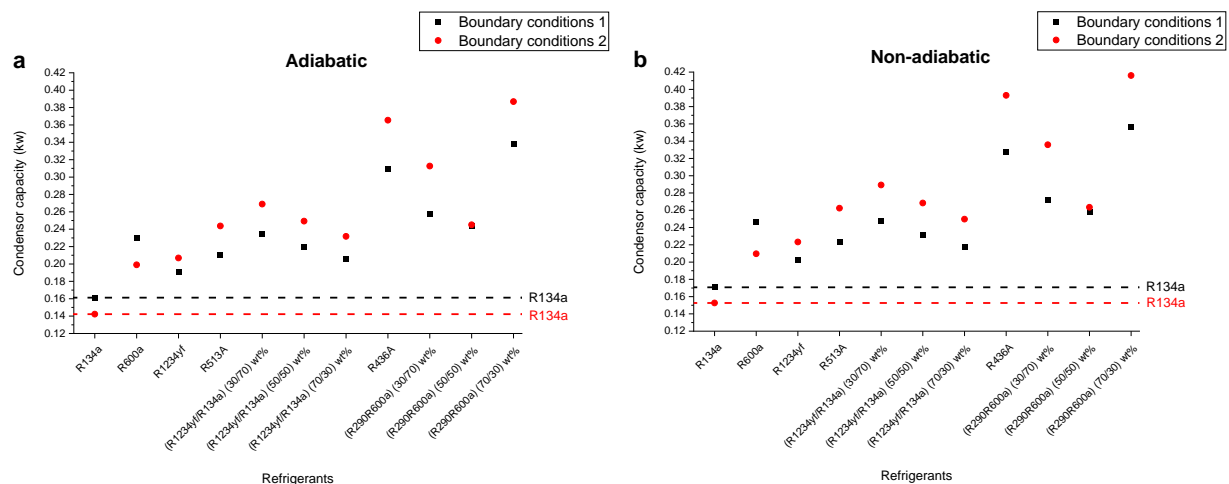

Figure 5. Condenser capacity Boundary conditions 1 and 2: a) Adiabatic, b) non-adiabatic

The power per ton of refrigeration (PPTR) for the different refrigerant combinations is shown in **Figure 6(a)**. The system's performance may be enhanced if the PPTR is low. **Figure 6(b)** shows that, compared to R22 and the other refrigerants that were investigated, the R134a, R1270, and R290 refrigerant combination (12 in Table 5) consumes less energy per refrigeration ton. As a result, combination 12 in Table 5 performs better than R22 and the other refrigerants that were researched. However, compared to all other refrigerants analyzed, R134a, R1270, and R419A refrigerants (6 and 22 in Table 5) had greater energy consumption per refrigeration ton. As a result, R134a, R1270, and R419A refrigerants have low coefficients of performance (COP). The power per ton of refrigeration (PPTR) for the different refrigerant mixtures is shown in **Figure 6(a)**. The system's performance may be enhanced if the PPTR is low. **Figure 6(b)** shows that the mixture of R134a, R1270, and R290 (12 in Table 5) uses less energy per refrigeration ton than R22 and the other refrigerants that were looked into. As a result, mixture 12 in Table 5 performs better than R22 and the other refrigerants that were researched. However, compared to all other refrigerants evaluated, R134a, R1270, and R419A refrigerants (6 and 22 in Table 5) had greater energy consumption per refrigeration ton. As a result, R134a, R1270, and R419A refrigerants have low coefficients of performance (COP). The values of the energy consumption factor per refrigeration ton (PPTR) under boundary condition 2 are shown in **Figures 6c** and d. The difference between the alternative mixtures with the base fluid R134a remains relatively small, however, indicating that these low operating conditions require a higher ability to circulate the fluid than the boundary conditions 1. In both cases, the compression is considered either adiabatic or non-adiabatic because it shows how the system acts at low temperatures (deep freeze), where the values of this factor are clearly higher than they are at the boundary conditions 1.
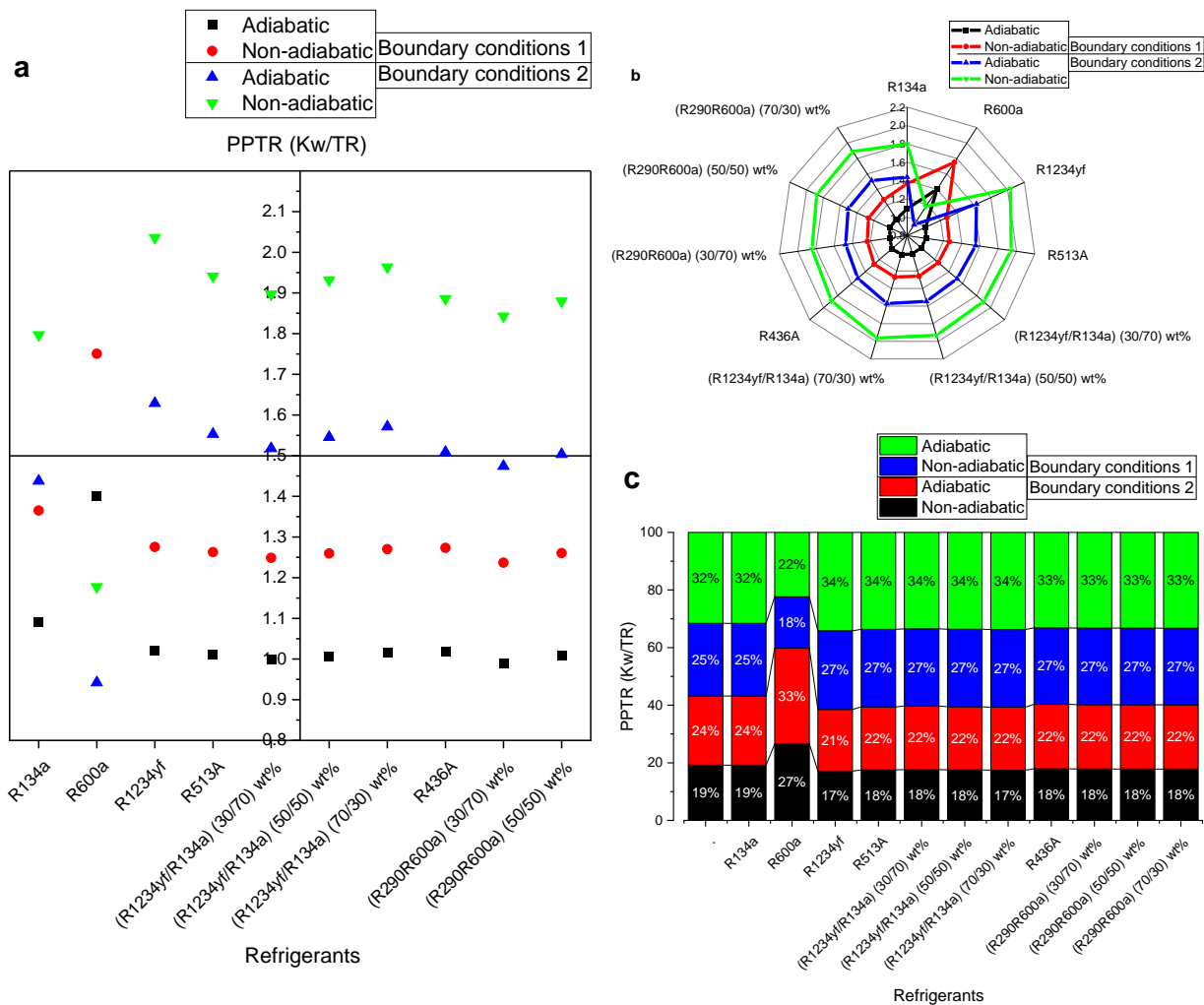
Figure 6. COP% - Adiabatic & non-adiabatic - Boundary conditions 1 and 2: a) scatter central, b) radar map, and c) stacked column

Figure 7 shows the cooling system's performance coefficient for adiabatic and non-adiabatic conditions, with Figures **7a** and **b** showing boundary conditions 1 and 2, respectively. The performance coefficient is considered the main indicator when evaluating how to choose the best refrigerant alternative. As a result, the coefficient of performance (COP) represents the system's Performance of the refrigeration cycle is the main consideration for selecting a new refrigerant as an alternative. When adiabatic compression is taken into consideration, it is obvious that the mixes in boundary condition 1 performed better than the main fluid, especially mixtures 10, 11, and 12, where the difference was between 0.65 and 0.89. Although the reality is that this improvement was less significant in non-adiabatic compression, it is still obvious, and the difference is between 0.18 and 0.26. This behavior is a result of the mixes' increased cooling capacities as compared to the base fluid as well as the compressor's specific operation rate, which is measured by the amount of thermal energy required to raise the fluid's pressure from low to high pressure. The capacity for cooling increases as the fluid's latent heat increases. As a consequence of the system requiring less compression work, its performance coefficient increased. The system's performance coefficient at boundary conditions 2 shows a very small improvement when we follow the behavior in **Figures 7b** and d, and it nearly does not change when we follow the behavior in the non-adiabatic approach. This is a result of the continuous elimination of thermal energy from the system under such deep cooling conditions. It lowers the internal system temperature, and deep cooling causes the cooling fluid's density to rise, requiring more energy to circulate the fluid at low temperatures (deep cooling). Even when the flow rate decreases, the energy needed to increase the pressure (the particular work of the compressor) is not considerably impacted. As a consequence, the COP values are noticeably lower than those for boundary condition 1. The variations in thermal performance between the mixes and the basic fluid are shown in **Figures 8a,** and **b**. This

demonstrates how the system responded to heat. In both adiabatic and non-adiabatic conditions, mixture No. 10 underperformed the base fluid by 10.35%. Procedure for compression at operating conditions 1 and lower In both adiabatic and non-adiabatic conditions, the performance for the same mixture increased by -2.4 in comparison to the base fluid for boundary conditions 2.
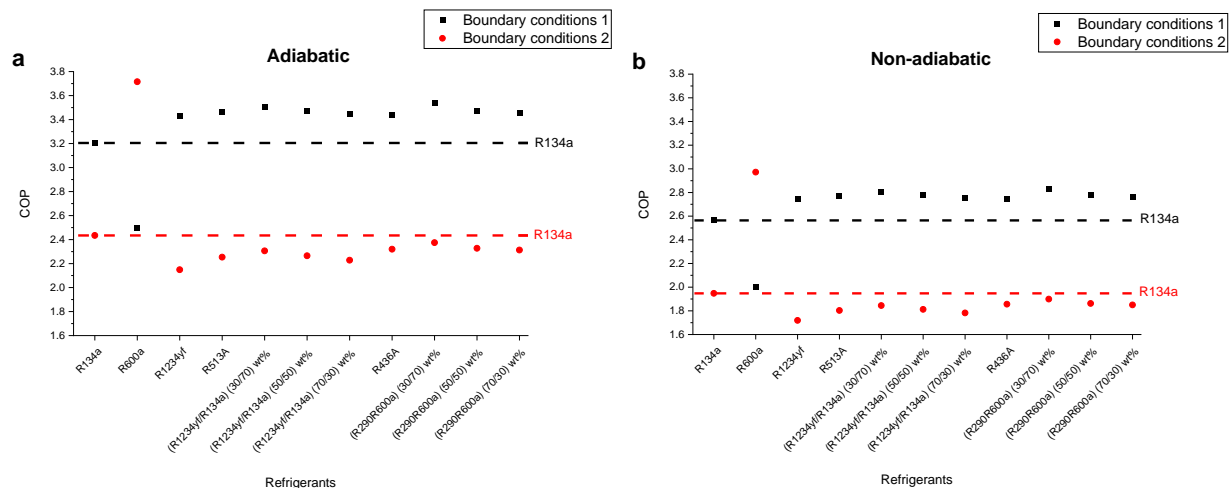

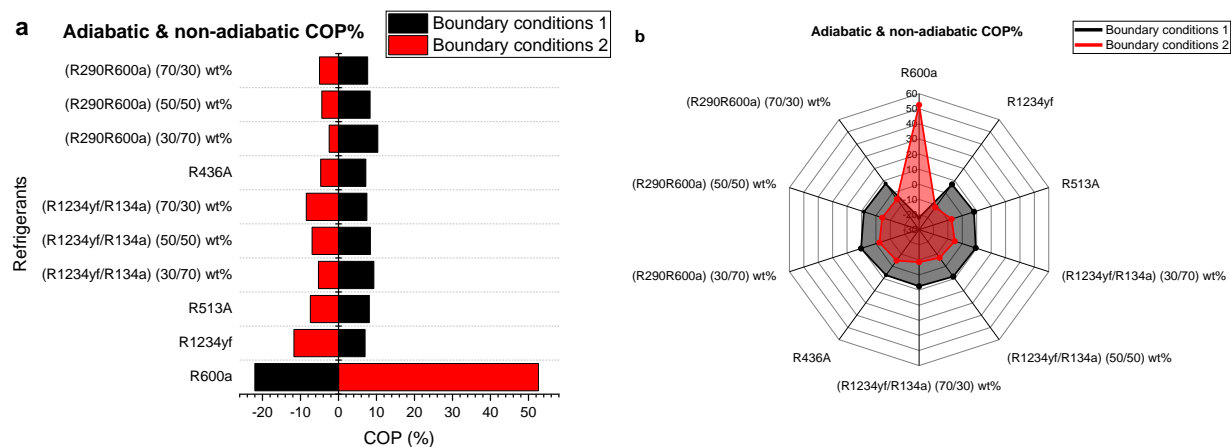Figure 7. COP Boundary conditions 1 and 2: a) Adiabatic, b) non-adiabatic

Figure 8. COP% - Adiabatic & non-adiabatic - Boundary conditions 1 and 2: a) population primed, b) radar map

9. Conclusions

The suggested refrigerant combinations have lower global warming potential (GWP) than the basic refrigerant, potentially attracting alternative applications in heating and air conditioning despite potential energy and thermal performance issues.

The mixtures had slightly higher cooling capacities compared to the base refrigerant due to their high latent heat capacity, requiring less energy for the same cooling capacity, which makes the mixtures more efficient at low temperatures.

The study looked at how different fluids and mixtures worked in a vapor compression refrigeration system. It found that natural refrigerant mixtures worked well, with the condensing capacity going up by 0.08 to 0.186 kW and the condensation capacity going up by 0.11 to 50.2 kW.

The system's performance improves with low PPTR. Combination 12 outperforms case 22 and other refrigerants, while R134a, R1270, and R419A have higher energy consumption per refrigeration ton compared to other analyzed refrigerants.

The performance coefficient (COP) is a crucial indicator for selecting the best refrigerant alternative. It represents the system's performance in the refrigeration cycle. Mixes in boundary condition 1 performed better than the base refrigerant, particularly mixtures 10, 11, and 12, with a difference between 0.65 and 0.89. However,

the improvement was less significant in non-adiabatic compression.

Authors contributions

M.H.K. and S.M.N., were responsible for study design and revising; methodology, M.H.K., M.S.H., O.A.O., S.O.M. and S.M.N.; software, M.H.K., S.O.M. and S.M.N.; validation, M.H.K., M.S.H., O.A.O., S.O.M. and S.M.N.; investigation, M.H.K., M.S.H., O.A.O., S.O.M. and S.M.N.; data curation, M.H.K., M.S.H., O.A.O., S.O.M. and S.M.N.; writing—original draft preparation, M.H.K. and S.M.N.; visualization, M.H.K., M.S.H., O.A.O., S.O.M. and S.M.N. All authors have read and agreed to the published version of the manuscript.

Funding

This research received no external funding.

Competing interests

The authors declare that they have no known competing financial interests or personal relationships that could have appeared to influence the work reported in this paper.

Informed consent

Obtained.

Ethics approval

The Publication Ethics Committee of the Canadian Center of Science and Education.

The journal's policies adhere to the Core Practices established by the Committee on Publication Ethics (COPE).

Provenance and peer review

Not commissioned; externally double-blind peer reviewed.

Data availability statement

The data that support the findings of this study are available on request from the corresponding author. The data are not publicly available due to privacy or ethical restrictions.

Data sharing statement

No additional data are available.

Open access

Copyrights

References

Al-Oran, O., Shaban, N. A., Manna, R., Ayadi, O., A'saf, A., & Lezsovits, F. (2024). Performance study of parabolic trough solar collector using hybrid nanofluids under Jordanian weather conditions. *Journal of Thermal Analysis and Calorimetry*, 1-18. https://doi.org/10.1007/s10973-024-12961-8

Bolaji, B. O. (2014). *Influence Of Sub-Cooling On The Energy Performance Of Two Eco-Friendly R22 Alternative Refrigerants. 34*(2), 73-83. https://doi.org/10.4314/just.v34i2.9

Calleja-Anta, D., Nebot-Andrés, L., Catalán-Gil, J., Sánchez, D., Cabello, R., & Llopis, R. (2020). Thermodynamic screening of alternative refrigerants for R290 and R600a. *Results in Engineering, 5*, 100081. https://doi.org/10.1016/j.rineng.2019.100081

Corr, E. G. (1995). Societal Transformation for Peace in El Salvador. *The ANNALS of the American Academy of Political and Social Science, 541*(1). https://doi.org/10.1177/0002716295541001010

Dalkilic, A. S., & Wongwises, S. (2010). A performance comparison of vapour-compression refrigeration system using various alternative refrigerants. *International Communications in Heat and Mass Transfer, 37*(9), 1340-1349. https://doi.org/10.1016/j.icheatmasstransfer.2010.07.006

Ewl, Ihb, MH, & MML. (2018). *REFPROP Documentation.*

Fatouh, M. (2018). Energy and exergy analysis of a household refrigerator using a ternary hydrocarbon mixture in tropical environment- Effects of refrigerant charge and capillary length. *Applied Thermal Engineering.* https://doi.org/10.1016/j.applthermaleng.2018.09.008

Gebbie, J. G., Jensen, M. K., Domanski, P. A., & Didion, D. A. (2004). Experimental pure fluid and binary mixture performance in a heat pump equipped with a distillation column. *International Journal of Refrigeration, 27*(8), 940-947. https://doi.org/10.1016/j.ijrefrig.2004.05.003

Graziosi, F., Arduini, J., Furlani, F., Giostra, U., Kuijpers, L. J. M., Montzka, S. A., Miller, B. R., O'Doherty, S. J., Stohl, A., Bonasoni, P., & Maione, M. (2015). European emissions of HCFC-22 based on eleven years of high frequency atmospheric measurements and a Bayesian inversion method. *Atmospheric Environment, 112*, 196-207. https://doi.org/10.1016/j.atmosenv.2015.04.042

Hamadalla, M. W., Jumaah, O. M., Mohamed, S. J., Karash, E. T., & Khaleel, M. H. (2023). Enhanced Performance of Vapor Compression Air Conditioners Using TiO2 Nanoparticle-Oil Additives. *International Journal of Heat and Technology, 41*(6), 1554-1560. https://doi.org/10.18280/ijht.410617

Hashimoto, M., Otsuka, T., Fukushima, M., Okamoto, H., Hayamizu, H., Ueno, K., & Akasaka, R. (2019). Development of New Low-GWP Refrigerants-Refrigerant Mixtures Including HFO-1123. *Science and Technology for the Built Environment, 25*(6), 776-783. https://doi.org/10.1080/23744731.2019.1603779

Kamel, M. S., & Najm, S. M. (2020). Heat transfer and fluid flow over a bank of circular tubes heat exchanger using nanofluids: CFD simulation. *IOP Conference Series: Materials Science and Engineering, 928*(2). https://doi.org/10.1088/1757-899X/928/2/022017

Karlsson, I., Rootzén, J., & Johnsson, F. (2020). Reaching net-zero carbon emissions in construction supply chains-Analysis of a Swedish road construction project. *Renewable and Sustainable Energy Reviews, 120*, 109651. https://doi.org/10.1016/j.rser.2019.109651

Khaleel, M. H., Khalefa, R. A. et al. (2018). Experimental performance investigation of domestic refrigerator charged by R600a and R134a. *Journal of University of Babylon for Engineering Sciences, 26*(9), 26-34.

Khalifaa, A. H. N., Faraja, J. J., & Khaleelb, M. H. (2017). Performance Study of Two Circuits Lorenz--Mutzner Vapour Compression Cycle. *Int. J. of Thermal & Environmental Engineering, 15*(2), 97-102.

Lund, H. (2007). Renewable energy strategies for sustainable development. *Energy, 32*(6), 912-919. https://doi.org/10.1016/j.energy.2006.10.017

McLinden, M. O., Seeton, C. J., & Pearson, A. (2020). New refrigerants and system configurations for vapor-compression refrigeration. *Science, 370*(6518), 791-796. https://doi.org/10.1126/science.abe3692

Nawaz, K., Shen, B., Elatar, A., Baxter, V., & Abdelaziz, O. (2017). R290 (propane) and R600a (isobutane) as natural refrigerants for residential heat pump water heaters. *Applied Thermal Engineering, 127*, 870-883. https://doi.org/10.1016/j.applthermaleng.2017.08.080

Park, K. J., & Jung, D. (2009). Performance of heat pumps charged with R170/R290 mixture. *Applied Energy, 86*(12), 2598-2603. https://doi.org/10.1016/j.apenergy.2009.04.009

Rasti, M., Ban, J. H., & Jeong, J. H. (2017). Development of a continuous empirical correlation for refrigerant mass flow rate through non-adiabatic capillary tubes. *Applied Thermal Engineering, 127*, 547-558. https://doi.org/10.1016/j.applthermaleng.2017.08.070

Reddy, D. V. R., Bhramara, P., & Govindarajulu, K. (2016). Hydrocarbon Refrigerant mixtures as an alternative to R134a in Domestic Refrigeration system: The state-of-the-art review. *International Journal of Scientific & Engineering Research, 7*(6), 87.

Rostamzadeh, H., Rostamzadeh, J., Matin, P. S., & Ghaebi, H. (2018). Novel dual-loop bi-evaporator vapor compression refrigeration cycles for freezing and air-conditioning applications. *Applied Thermal Engineering, 138*, 563-582. https://doi.org/10.1016/j.applthermaleng.2018.04.085

Sahaym, U., & Norton, M. G. (2008). Advances in the application of nanotechnology in enabling a 'hydrogen economy'. *Journal of Materials Science, 43*(16), 5395-5429. https://doi.org/10.1007/s10853-008-2749-0

Shaik, S. V., & Babu, T. P. A. (2017). Theoretical Performance Investigation of Vapour Compression Refrigeration System Using HFC and HC Refrigerant Mixtures as Alternatives to Replace R22. *Energy Procedia, 109*(November 2016), 235-242. https://doi.org/10.1016/j.egypro.2017.03.053

Wang, S. K. (1994). *Handbook of air conditioning and refrigeration.* In Choice Reviews Online (Vol. 32, Issue 02). https://doi.org/10.5860/choice.32-0959

Yang, Z., Feng, B., Ma, H., Zhang, L., Duan, C., Liu, B., Zhang, Y., Chen, S., & Yang, Z. (2021). Analysis of lower GWP and flammable alternative refrigerants. *International Journal of Refrigeration, 126*, 12-22.

Appendixes

Appendixes A:

Table A1. Evaluation cases with both adiabatic and non-adiabatic conditions

Refrigerant	Case1		Case2		Case3		Case4	
R134a	Non-adiabatic	Condition -1-	adiabatic	Condition -1-	Non-adiabatic	Condition -2-	adiabatic	Condition -2-
Refrigerant	Case5		Case6		Case7		Case8	
R600a	Non-adiabatic	Condition -1-	adiabatic	Condition -1-	Non-adiabatic	Condition -2-	adiabatic	Condition -2-
Refrigerant	Case9		Case10		Case11		Case12	
R290	Non-adiabatic	Condition -1-	adiabatic	Condition -1-	Non-adiabatic	Condition -2-	adiabatic	Condition -2-
Refrigerant	Case13		Case14		Case15		Case16	
R1234yf	Non-adiabatic	Condition -1-	adiabatic	Condition -1-	Non-adiabatic	Condition -2-	adiabatic	Condition -2-
Refrigerant	Case17		Case18		Case19		Case20	
R513A(56/44)wt%(R1234yf/R134a)	Non-adiabatic	Condition -1-	adiabatic	Condition -1-	Non-adiabatic	Condition -2-	adiabatic	Condition -2-
Refrigerant	Case21		Case22		Case23		Case24	
(30/70) wt%(R1234yf/R134a)	Non-adiabatic	Condition -1-	adiabatic	Condition -1-	Non-adiabatic	Condition -2-	adiabatic	Condition -2-
Refrigerant	Case25		Case26		Case27		Case28	
(50/50) wt%(R1234yf/R134a)	Non-adiabatic	Condition -1-	adiabatic	Condition -1-	Non-adiabatic	Condition -2-	adiabatic	Condition -2-
Refrigerant	Case29		Case30		Case31		Case32	
(70/30) wt%(R1234yf/R134a)	Non-adiabatic	Condition -1-	adiabatic	Condition -1-	Non-adiabatic	Condition -2-	adiabatic	Condition -2-
Refrigerant	Case33		Case34		Case35		Case36	
R436A(54/46)wt%(R290R600a)	Non-adiabatic	Condition -1-	adiabatic	Condition -1-	Non-adiabatic	Condition -2-	adiabatic	Condition -2-
Refrigerant	Case37		Case38		Case39		Case40	
(30/70)wt%(R290R600a)	Non-adiabatic	Condition -1-	adiabatic	Condition -1-	Non-adiabatic	Condition -2-	adiabatic	Condition -2-
Refrigerant	Case41		Case42		Case43		Case44	
(50/50)wt%(R290R600a)	Non-adiabatic	Condition -1-	adiabatic	Condition -1-	Non-adiabatic	Condition -2-	adiabatic	Condition -2-
Refrigerant	Case45		Case46		Case47		Case48	
(70/30)wt%(R290R600a)	Non-adiabatic	Condition -1-	adiabatic	Condition -1-	Non-adiabatic	Condition -2-	adiabatic	Condition -2-

Table A2. Thermodynamic properties of refrigerants vs cases (1 to 12) of evaluations

Property/ No of Case	Case1	Case2	Case3	Case4	Case5	Case6	Case7	Case8	Case9	Case10	Case11	Case12
Pel (barg)	0.626	0.626	0.0507	0.0507	-0.428	-0.428	-0.1227	-0.1227	1.9030	1.9030	1.021	1.021
Pev (barg)	0.626	0.626	0.0507	0.0507	-0.428	-0.428	-0.1227	-0.1227	1.9030	1.9030	1.021	1.021
hel (kJ/kg)	180.14	180.14	167.19	167.19	144.43	144.43	166.29	166.29	163.28	163.28	139.6	139.6
hev (kJ/kg)	389.63	389.63	383.45	383.45	520.99	520.99	534.26	534.26	557.93	557.93	546.28	546.28
Pcl (barg)	10.586	10.586	10.586	10.586	5.0312	5.0312	4.298	4.298	12.681	12.681	14.33	14.33
Pcv (barg)	10.586	10.586	10.586	10.586	5.0312	5.0312	4.298	4.298	12.681	12.681	14.33	14.33
hcl (kJ/kg)	238.84	238.84	263.94	263.94	309.07	309.07	607.80	607.80	307.15	307.15	321.79	321.79
hcv (kJ/kg)	413.84	413.84	421.52	421.52	614.34	614.34	534.26	534.26	614.21	614.21	618.12	618.12
h1 (kJ/kg)	393.8	393.8	386..64	386..64	526.9	526.9	541.94	541.94	566.03	566.03	552.49	552.49
υ1 (m3/kg)	0.1236	0.1236	0.18512	0.18512	0.6002	0.6002	0.4077	0.4077	0.15766	0.15766	0.220	0.220
S1=s2 (kJ/kg.C)	1.7531	1.7531	1.7589	1.7589	2.3282	2.3282	2.328	2.328	2.4229	2.4229	2.4338	2.4338
h2s (kJ/kg)	435.74	435.74	437.67	437.67	615.09	615.09	610.10	610.10	640.69	640.69	649.89	649.89
h2 (kJ/kg)	446.225	-	450.42	-	637.137	-	627.14	-	659.35	-	674.24	-
h3=h4 (kJ/kg)	259.39	259.39	262.42	262.42	306.50	306.50	288.71	288.71	298.48	298.48	318.81	318.81

Table A3. Thermodynamic properties of refrigerants vs cases (13 to 24) of evaluations

Property/ No of Case	Case13	Case14	Case15	Case16	Case17	Case18	Case19	Case20	Case21	Case22	Case23	Case24
Pel (barg)	0.823	0.823	0.2153	0.2153	1.0316	1.0316	0.34907	0.34907	0.9448	0.9448	0.28421	0.28421
Pev (barg)	0.823	0.823	0.2153	0.2153	1.0296	1.0296	0.34592	0.34592	0.88129	0.88129	0.23034	0.23034
hel (kJ/kg)	17.601	17.601	5.376	5.376	94.827	94.827	82.263	82.263	136.2	136.2	123.46	123.46
hev (kJ/kg)	189.97	189.97	183.27	183.27	277.2	277.2	270.87	270.87	329.33	329.33	323.10	323.10
Pcl (barg)	9.1707	9.1707	10.525	10.525	10.486	10.486	12.028	12.028	10.262	10.262	11.796	11.796
Pcv (barg)	9.1707	9.1707	10.525	10.525	10.483	10.483	12.024	12.024	10.176	10.176	11.711	11.711
hcl (kJ/kg)	91.418	91.418	98.875	98.875	170.28	170.28	177.85	177.85	212.13	212.13	219.71	219.71
hcv (kJ/kg)	223.75	223.75	226.24	226.24	307.78	307.78	309.86	309.86	359.18	359.18	361.2	361.2
h1 (kJ/kg)	194.32	194.32	186.59	186.59	281.5	281.5	274.17	274.17	333.58	333.58	326.35	326.35

Property												
υ1 (m3/kg)					0.09206	0.09206	0.1348	0.1348	0.10276	0.10276	0.1524	0.1524
S1=s2 (kJ/kg.C)	0.75431	0.75431	0.75527	0.75527	1.2329	1.2329	1.2338	1.2338	1.49	1.49	1.4934	1.4934
h2s (kJ/kg)	225.59	225.59	228.11	228.11	314.9	314.9	317.59	317.59	369.53	369.53	373.26	373.26
h2 (kJ/kg)	233.40	-	238.49	-	323.25	-	328.445	-	378.517	-	384.987	-
h3=h4 (kJ/kg)	87.089	87.089	97.371	97.371	165.78	165.78	176.31	176.31	207.63	207.63	218.17	218.17

Table A4. Thermodynamic properties of refrigerants vs cases (25 to 36) of evaluations

Property/ No of Case	Case25	Case26	Case27	Case28	Case29	Case30	Case31	Case32	Case33	Case34	Case35	Case36
Pel (barg)	1.0228	1.0228	0.34184	0.34184	1.0254	1.0254	0.3479	0.3479	1.1070	1.1070	0.45482	0.45482
Pev (barg)	1.0117	1.0117	0.33036	0.33036	1.0188	1.0188	0.34447	0.34447	0.57331	0.57331	0.04856	0.04856
hel (kJ/kg)	104.65	104.65	92.046	92.046	71.25	71.25	58.786	58.786	164.74	164.74	141.94	141.94
hev (kJ/kg)	289.19	289.19	282.89	282.89	249.34	249.34	242.91	242.91	549.46	549.46	536.75	536.75
Pcl (barg)	10.489	10.489	12.036	12.036	10.34	10.34	11.853	11.853	9.2234	9.2234	10.472	10.472
Pcv (barg)	10.488	10.488	12.036	12.036	10.281	10.281	11.786	11.786	7.7099	7.7099	8.8603	8.8603
hcl (kJ/kg)	180.24	180.24	187.82	187.82	146.31	146.31	153.85	153.85	301.66	301.66	315.33	315.33
hcv (kJ/kg)	319.51	319.51	321.56	321.56	280.73	280.73	282.91	282.91	616.50	616.50	622.04	622.04
h1 (kJ/kg)	293.49	293.49	286.18	286.18	253.67	253.67	246.22	246.22	549.45	549.45	542.76	542.76
υ1 (m3/kg)	0.0935	0.0935	0.1374	0.1374	0.09105	0.09105	0.1327	0.1327	0.26047	0.26047	0.3859	0.3859
S1=s2 (kJ/kg.C)	1.2933	1.2933	1.2947	1.2947	1.0397	1.0397	1.0894	1.0894	2.3837	2.3837	2.4222	2.4222
h2s (kJ/kg)	327.39	327.39	330.29	330.29	286.14	286.14	288.37	288.37	623.92	623.92	641.98	641.98
h2 (kJ/kg)	335.865	-	341.317	-	294.25	-	298.9	-	642.537	-	666.785	-
h3=h4 (kJ/kg)	175.74	175.74	186.27	186.27	141.84	141.84	152.32	152.32	293.58	293.58	312.57	312.57

Table A5. Thermodynamic properties of refrigerants vs cases (37 to 48) of evaluations

Property/ No of Case	Case37	Case38	Case39	Case40	Case41	Case42	Case43	Case44	Case45	Case46	Case47	Case48
Pel (barg)	0.57789	0.57789	0.076034	0.076034	0.98888	0.98888	0.37039	0.37039	1.3741	1.3741	0.64543	0.64543
Pev (barg)	0.18207	0.18207	0.22243	0.22243	0.46838	0.46838	-0.024763	-0.024763	0.86582	0.86582	0.25547	0.25547
hel (kJ/kg)	165.5	165.5	143.16	143.16	164.92	164.92	142.23	142.23	164.3	164.3	141.24	141.24
hev (kJ/kg)	542.4	542.4	529.37	529.37	547.89	547.89	535.09	535.09	552.86	552.86	540.39	540.39
Pcl (barg)	7.0482	7.0482	8.062	8.062	8.7312	8.7312	9.9257	9.9257	10.353	10.353	11.728	11.728
Pcv (barg)	5.8750	5.8750	6.8074	6.8074	7.2366	7.2366	8.3323	8.3323	8.9632	8.9632	10.253	10.253
hcl (kJ/kg)	298.98	298.98	312.2	312.2	301.01	301.01	314.57	314.57	303.26	303.26	317.2	317.2
hcv (kJ/kg)	613.09	613.09	619.19	619.19	615.90	615.90	621.58	621.58	617.3	617.3	622.44	622.44
h1 (kJ/kg)	550.15	550.15	535.33	535.33	555.69	555.69	541.09	541.09	560.74	560.74	546.45	546.45
υ1 (m3/kg)	0.3311	0.3311	0.48461	0.48461	0.28122	0.28122	0.40852	0.40852	0.23208	0.23208	0.33365	0.33365
S1=s2 (kJ/kg.C)	2.3802	2.3802	2.3851	2.3851	2.4072	2.4072	2.415	2.415	2.4252	2.4252	2.4352	2.4352
h2s (kJ/kg)	623.38	623.38	630.43	630.43	631.37	631.37	639.58	639.58	637.73	637.73	646.79	646.79
h2 (kJ/kg)	641.6875	-	654.205	-	650.29	-	664.202	-	656.9775	-	671.875	-
h3=h4 (kJ/kg)	291.16	291.16	309.54	309.54	292.99	292.99	311.84	311.84	295.02	295.02	314.38	314.38

Appendixes B:

Table B1. Thermophilic properties for mass flow calculations vs refrigerants cases (1 to 16)

Property (units)	Case1+ Case2 R134a	Case3+ Case4 R134a	Case5+Case6 (R600a)	Case7+Case8 (R600a)	Case9+Case10 (R290)	Case11+Case12 (R290)	Case13+Case14 (R1234yf)	Case15+Case16 (R1234yf)
Tc,in (K)	310	317	317	310	310	317	310	317
Ts,in (K)	263	252	252	263	263	252	263	252
Pc,in (Pa)	1158600	1158600	603120	529800	1368100	1533000	1017070	1152500
Ps,in (Pa)	162600	105070	57200	87730	290300	202100	182300	121530
μfc (Pa.s)	0.00016804	0.00015366	0.00012441	0.00013364	0.000085717	0.000079408	0.00013504	0.00012404
ϑfc (m³.kg⁻¹)	0.00086213	0.00088485	0.0019013	0.0018678	0.0021144	0.0021714	0.00095548	0.00098270
hc,in (J. kg⁻¹)	259390	437670	306500	288710	298480	318810	87089	97371
hf (J. kg⁻¹)	251730..	262200.	306110.	288320.	298100.	318390.	86891.	97160.
hfg (J. kg⁻¹)	166300	158850	306730	315330	313500	29886	86891	128520
ΔTsh (K)	5	4	4	5	5	4	5	4
CPfc (J.Kg⁻¹)	1480.7	1522.2	2564.6	2511.6	2866.4	2974.7	1454.0	1499.1
m_{fc} (Kgs⁻¹) ×10⁻⁴	9.140299	8.118798	7.456102	6.193441	10.50869	15.02144	13.80668	15.82365

Table B2. Thermophilic properties for mass flow calculations vs refrigerants cases (17 to 32)

Property (units)	Case17+Case18 R513A	Case19+Case20 R513A	Case21+Case22 (R134a+R1234yf) (70%+30%)	Case23+Case24 (R134a+R1234yf) (70%+30%)	Case25+Case26 (R134a+R1234yf) (50%+50%)	Case27+Case28 (R134a+R1234yf) (50%+50%)	Case29+Case30 (R134a+R1234yf) (30%+70%)	Case31+Case32 (R134a+R1234yf) (30%+70%)
T_c,in (K)	310	317	310	317	310	317	310	317
T_s,in (K)	263	252	263	252	263	252	263	252
P_c,in (Pa)	1148600	1302800	1126200	1279600	1148900	1303600	1134000	1285300
P_s,in (Pa)	229600	134592	188120	123034	201170	133036	201880	134470
μ_{fc} (Pa.s)	0.00013871	0.00012668	0.00014883	0.00013588	0.00014051	0.00012830	0.00013572	0.00012410
ϑ_{fc} (m^3.kg^{-1})	0.00093249	0.00096065	0.00090367	0.00092986	0.00092667	0.00095452	0.00094373	0.00097222
h_c,in (J. kg^{-1})	165780	176310	207630	218170	175740	186270	141840	152321
h_f (J. kg^{-1})	165590.	176100.	207430.	217950.	175540.	186060.	141640.	152110.
h_{fg} (J. kg^{-1})	140790	133300	150390	142810	142590	135050	137630	130310
ΔT_{sh} (K)	5	4	5	4	5	4	5	4
CP_{fc} (J.Kg^{-1})	1488.5	1540.1	1490.0	1538.6	1490.0	1541.3	1481.9	1533.0
m_{fc} (Kg.s^{-1}) ×10^{-4}	14.14144	17.25036	14.46225	17.33955	14.48362	17.3093	14.28364	17.03263

Table B3. Thermophysical properties for mass flow calculations vs refrigerants cases (33 to 48)

Property (units)	Case33+Case34 R436A	Case35+Case36 R436A	Case37+Case38 (R290+R600a) (30%+70%)	Case39+Case40 (R290+R600a) (30%+70%)	Case41+Case42 (R290+R600a) (50%+50%)	Case43+Case44 (R290+R600a) (50%+50%)	Case45+Case46 (R290+R600a) (70%+30%)	Case47+Case48 (R290+R600a) (70%+30%)
T_c,in (K)	310	317	310	317	310	317	310	317
T_s,in (K)	263	252	263	252	263	252	263	252
P_c,in (Pa)	1022340	1147200	804820	906200	973120	1092570	1135300	1272800
P_s,in (Pa)	157331	104856	118207	77757	823660	97523.7	186582	125547
μ_{fc} (Pa.s)	0.00010274	0.000095607	0.00011526	0.00010735	0.00010542	0.000098135	0.000096863	0.000090053
ϑ_{fc} (m^3.kg^{-1})	0.0019973	0.0020417	0.0019353	0.0019741	0.0019826	0.0020256	0.0020326	0.0020804
h_c,in (J. kg^{-1})	293580	312570	291160	309540	292990	311840	295020	314380
h_f (J. kg^{-1})	293170.	312160.	290750.	309140.	292590.	311430.	294610.	313970.
h_{fg} (J. kg^{-1})	319770	308620	580150	308650	319660	308860	319350	307310
ΔT_{sh} (K)	5	4	5	4	5	4	5	4
CP_{fc} (J.Kg^{-1})	2678.4	2752.6	2593.3	2655.9	2657.4	2728.5	2731.1	2813.6
m_{fc} (Kg.s^{-1}) ×10^{-4}	9.371069	11.09456	7.751085	9.742569	7.21762	7.47773	9.855987	11.63736